The Reaction of Permanganyl Chloride with Olefins: Intermediates and Mechanism as Derived from Matrix-Isolation Studies and Density Functional Theory Calculations

Tobias Wistuba and Christian Limberg*[a]

Dedicated to Professor Hansgeorg Schnöckel on the occasion of his 60th birthday

Abstract: Density functional theory (DFT) calculations predict that the [2+3] addition of tetramethylethylene (TME) to the MnO_2 moiety of MnO_3Cl is thermodynamically favoured over [2+1] addition (epoxidation), while the kinetic barriers for both reactions are of comparable height. However, in an experimental investigation of the TME/MnO_3Cl system by means of matrix-isolation techniques, selective formation of the epoxidation product [ClO_2Mn-{$O[C(CH_3)_2]_2$}] (**1**) was observed. Compound **1** was characterised by IR spectroscopy with the aid of isotopic-enrichment experiments in combination with DFT frequency calculations. This result, at first sight surprising, is supported by studies in solution, and, even with the numerically equal energy barriers suggested by the calculations, it can be rationalised in terms of the much broader reaction channel leading to epoxidation as opposed to the much more narrow approach path for formation of the glycolate.

Keywords: density functional calculations · epoxidation · manganese · matrix isolation · oxidation

Introduction

Transition metal oxides and their complexes play pivotal roles in numerous important biological and nonbiological, stoichiometric and catalytic processes in which oxo groups are transferred to organic substrates.[1–5] For instance, simple d^0-metal–oxo compounds and oxometal halides such as CrO_2Cl_2,[6, 7] OsO_4[8, 9] MnO_4^-[10–12] are applied extensively in reactions in which oxygen is inserted into a C–H bond or undergoes addition to an olefinic double bond. The widespread practical use of such reagents has spurred considerable interest in the underlying activation mechanisms,[1–4, 8, 13–16] and kinetic studies date back to the 1940s. However, although intense research in this area has provided a broad synthetic, structural and mechanistic basis, many of the key steps remain unknown, and some of the reasons for this are the high and complex reactivities, diverse reaction pathways and the heterogeneity of the inorganic reduction products, which thus elude characterisation. In the last five or six years investigations into the reaction mechanisms of simple metal–oxo compounds and oxometal halides have been intensified again,[17–30] as it was recognised that the combination of methods available today (elaborate quantum-mechanical calculations, matrix-isolation and gas-phase techniques, as well as sophisticated kinetic studies) allows deeper insights into these systems.[31] For example, the reinvestigation of the system MnO_4^-/alkylaromatic compounds considerably improved the understanding of the reactivity principles characteristic of permanganate oxidations and led to a new way of thinking about d^0-metal–oxo compounds in general.[19, 20]

The reaction of permanganate with olefins recently received renewed interest, too. The results of DFT calculations[30] strongly support the original idea[14] that permanganate dihydroxylations follow the [3+2] cycloaddition mechanism established earlier for OsO_4[26] and exclude a stepwise process involving a [2+2] cycloaddition (Scheme 1). The concerted [2+3] pathway was found to be favoured by not less than 173 kJ mol^{-1}. The fact that the reaction rates are influenced differently by donor and acceptor olefins on going from OsO_4 to MnO_4^- was attributed to charge differences.

It would be of interest to isolate and study the primary intermediates of such reactions directly, for instance, with the aid of matrix-isolation techniques, which only recently served to identify elusive intermediates of the system CrO_2Cl_2/olefin.[22, 23, 31] However, the reactions of permanganate cannot

[a] Priv.-Doz. Dr. C. Limberg, T. Wistuba
Anorganisch-Chemisches Institut
Universität Heidelberg
Im Neuenheimer Feld 270
69120 Heidelberg
Fax: (+49) 6221-545707
E-mail: limberg@sun0.urz.uni-heidelberg.de

Supporting information for this article is available on the WWW under http://wiley-vch.de/home/chemistry/ or from the author.

0947-6539/01/0721-4674 $ 17.50+.50/0

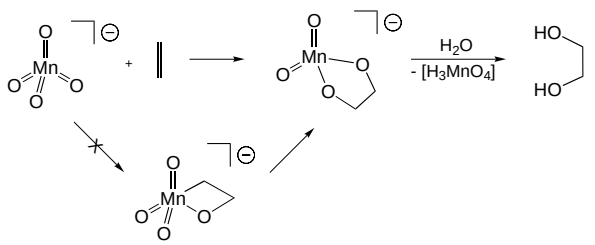

Scheme 1. Reaction mechanism postulated for the oxidation of olefins with MnO_3Cl.

be investigated by this method, as permanganate salts are not volatile enough to allow their embedment in low-temperature noble gas matrices. However, a neutral derivative of the permanganate ion with sufficient volatility is available: permanganyl chloride MnO_3Cl. Its existence was first postulated in 1827, but it was not until 1968 that its identity was confirmed unequivocally.[32] Subsequently, its spectroscopic properties (IR, UV/Vis and photoelectron-spectroscopy, as well as magnetic circular dichroism) were investigated in detail,[33] but, probably because it is difficult to handle owing to its extreme oxidative power, hydrolytic sensitivity, and instability above $-30\,^{\circ}C$, no reports on its reactivity with respect to organic or inorganic compounds are available.

Bearing the above-mentioned mechanistic discussions concerning the reactivity of permanganate in mind, we were interested in studying the reactions of permanganyl chloride with olefins by means of matrix-isolation techniques in order to identify the primary products formed. The attention focused on thermally (and not photochemically) induced reactions, as these could then be analysed in comparison with the permanganate system, whereby the effect of replacing an O^{2-} by a Cl^- ligand is of interest.

Results and Discussion

Reaction of MnO_3Cl with $(CH_3)_2C{=}C(CH_3)_2$: The reactions of permanganyl chloride with olefins cannot be induced at temperatures below 50 K, which is the maximum temperature to which noble gas matrices (even with Xe coating) can be warmed without considerable loss of matrix quality. Therefore, the matrix assembly was designed such that it would allow reaction between MnO_3Cl and the olefin during the short period of the cocondensation process: MnO_3Cl and the olefin diluted by argon were sprayed onto a CsI window cooled to 7 K from two different nozzles, so that, after focussing, the beams followed a common path of 2 cm in the gas phase before they condensed. We thus hoped to quench any primary product formed by immediate isolation in an argon matrix at 7 K, and to identify it by IR spectroscopy.[34] Ethylene and propylene failed to react in this procedure: they could be matrix-isolated in unchanged form besides MnO_3Cl. However, the electron-rich tetramethylethylene (TME) showed a significant reaction. Systematic variation of the cocondensation rates and concentrations of the reagents to achieve the best possible matrix quality and an acceptable conversion lead to the following ideal experimental conditions: a 5% TME/Ar mixture was cocondensed with neat MnO_3Cl, whose deposition rate was regulated by maintaining the sample at $-65\,^{\circ}C$. To obtain information on isotopic shifts, which are very important for band assignments, the experiments were carried out not only with $^{16}O_3MnCl$ but also with $^{18}O_3MnCl$. The IR spectrum shown in Figure 1 was obtained with $^{18}O_3MnCl$. In comparison to the spectrum recorded after employment of $^{16}O_3MnCl$ it has the advantage of minimal band overlap, which substantially facilitated the computational subtraction of the absorption bands of the unconsumed starting materials. Bands of new products can thus be immediately recognized, and consequently the spectrum of the ^{18}O-enriched material is more instructive than that of its ^{16}O counterpart. The data for ^{16}O and ^{18}O are summarised in Table 1. The relative intensities of all product bands remained constant on variation of the experimental conditions (vide supra), and this suggests that they all belong to a single product. The most important region is that between 1000 and 700 cm^{-1}, where the Mn=O vibrations and certain C–O modes absorb, and three major product bands can recognized there: The most prominent band is at 898 cm^{-1} with a $\Delta(^{16}O/^{18}O)$ of 39 cm^{-1}, a weaker band at 818 cm^{-1} ($\Delta(^{16}O/^{18}O) = 52$ cm^{-1}) and a further intense band at 782 cm^{-1} ($\Delta(^{16}O/^{18}O) = 27$ cm^{-1}). To identify the corresponding product, the structures of all reasonable species were calculated (DFT), and their vibrational frequencies were compared with the experimental data.

Calculations: Density functional calculations are more suitable than ab initio methods for frequency calculations on metal–oxo species.[35] Calculations on the products resulting from the CrO_2Cl_2/olefin system further established that at the B3LYP/LanL2DZ level of theory[22, 23] deviations of 100 cm^{-1} are not unusual and have their origins in very small differences between the theoretical and real structures.[22, 23, 36] However, in each case considered, the general band pattern was in accordance with the experimental one.[22, 23] Our theoretical investigation therefore started with the functional/basis set combination B3LYP/LanL2DZ, but as problems were encountered in the calculations on transition states (vide infra), we switched to the computationally more demanding basis set 6-311G(d), which is considered to be slightly superior for metal–oxo compounds.[37] The entire study was performed at the B3LYP/6-311G(d) level, which has been shown in many cases to represent a reliable combination of functional and basis set for organometallic compounds.[30b] Its known tendency to overestimate the fundamental vibrations of metal–oxo cores, however, must be borne in mind.[37]

The system MnO_3Cl/TME: product identification: Attempts were made to optimise the structures of the potential products depicted in Scheme 2 (B3LYP/6-311G(d)) in form of their singlet and triplet states with C_1 symmetry (see Table 2). Only **7**, which could conceivably be formed by proton-coupled electron transfer,[18, 19] was treated differently. It is a radical pair, and both radicals were investigated separately in form of their doublet states.

To identify the species responsible for the experimental IR absorptions, the calculated vibrational frequencies were

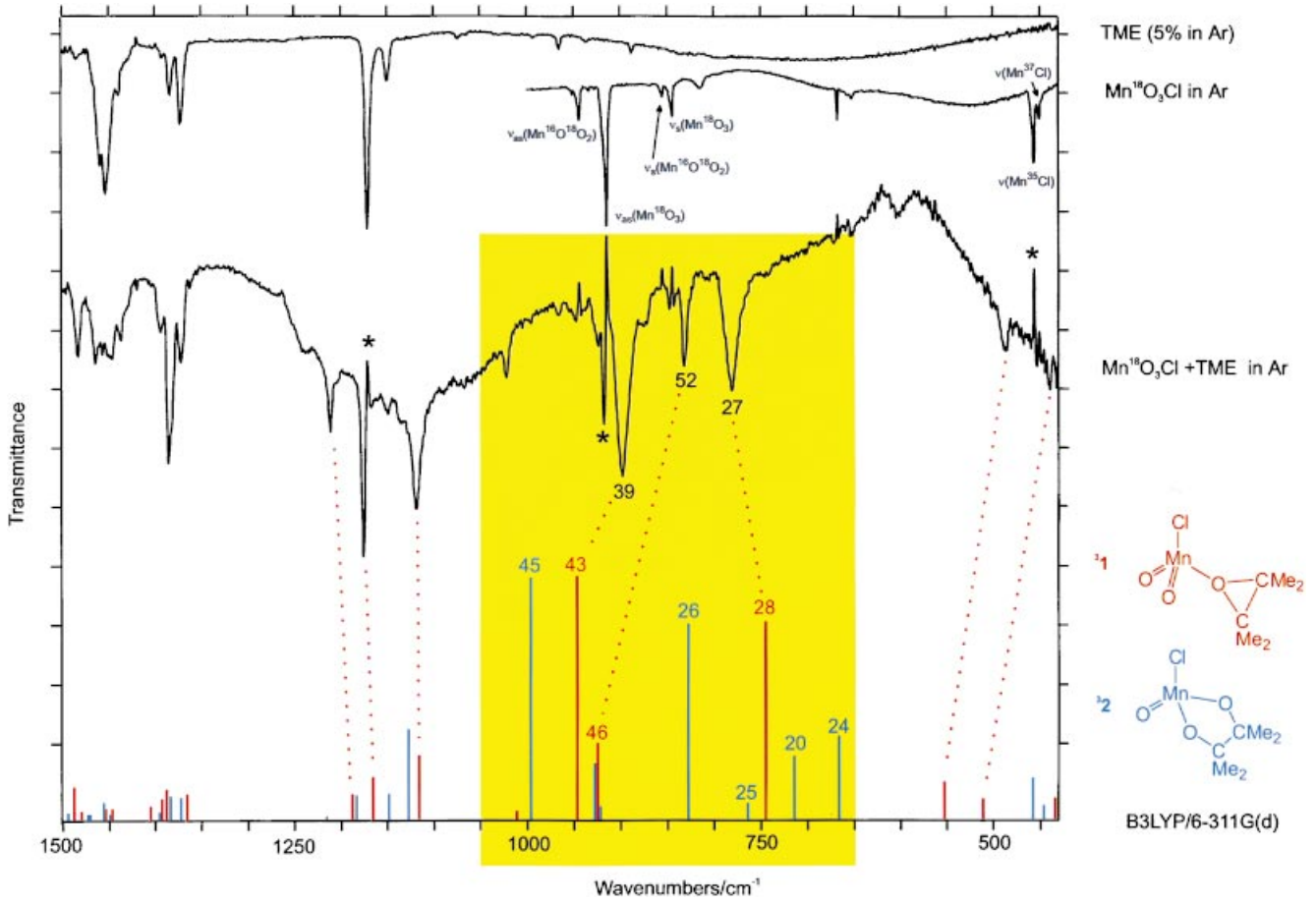

Figure 1. Upper trace: the spectrum of TME isolated in an argon matrix (5 mol%) at 7 K in the region between 430 and 1500 cm^{-1}. Middle trace: the spectrum of $Mn^{18}O_3Cl$ isolated in an argon matrix at 7 K in the region between 430 and 1000 cm^{-1}. Lower trace: the spectrum obtained after cocondensation of $Mn^{18}O_3Cl$ and TME/Ar at 7 K after weighted subtraction of the spectra of the starting materials (the asterisks denote bands (positive and negative) due to imperfect subtraction of the bands of the starting materials; they arise from slight band shifts due to different temperatures). Bottom: The line diagram calculated for the IR spectra of ^{3}**1** and ^{3}**2**, as shown in Figure 2, by means of DFT calculations at the B3LYP/6–311G(d) level (a scaling factor of 0.97 was applied).

considered. A scaling factor of 0.97 is accepted for B3LYP/6-311G(d) calculations[37] and was applied in the present study, too.

In contrast to the reactions with MnO_4^-, for which calculations were performed exclusively on the singlet potential energy surfaces (PESs),[30] crossovers to the triplet surfaces have to be considered in the case of MnO_3Cl. The MnO_3Cl/olefin system itself has a singlet ground state, and the addition of an olefin to the metal–oxo bonds can lead to a d^0 or a d^2 system. While d^0 systems (such as **3** and **6**) usually also have singlet ground states, the d^2 products (**1**, **2**, **4**, **5**) proved to be generally much more stable in their triplet states (vide infra and Table 2). The situation with MnO_3Cl is therefore more comparable to that of CrO_2Cl_2, for which the olefin oxidation products also have triplet ground states,[22–25] than to that of OsO_4, which reacts with olefins solely on the singlet surface.[26]

We failed to find a minimum corresponding to the geometry of the d^0 molecules ^{1}**3** or ^{3}**3** (the superscripts denote the singlet and triplet spin states) on the PES, probably because the Mn^{VII} centre of MnO_3Cl is very electron poor and hard (as opposed to that of the MnO_4^- ion) which has an additional electron, and therefore it is not capable of forming a reasonably strong Mn–C bond. On the singlet surface we were able to optimise a structure with a manganaoxetane-like geometry, namely, ^{1}**3*** (Scheme 2), but with a very long Mn–C distance (2.334 Å, as compared to 2.013 Å[30a] in the manganaoxetane derived from MnO_4^- and ethylene shown in Scheme 1; that is, the Mn–C bond is basically no longer intact). Accordingly, the Mn–C distance in the structure of ^{1}**6***, as optimised from a starting geometry corresponding to ^{1}**6**, is also very long (2.660 Å). The frequencies calculated for ^{1}**3*** are not in agreement with those of the experimental bands, as, for instance, an intense absorption was predicted at 630 cm^{-1} corresponding to a ν(Mn-O-C) vibration, while the region around 630 cm^{-1} is free of bands in the experimental spectrum.

The structure of ^{3}**4** could be optimised, and a subsequent frequency calculation predicted the most intense band (due to a $\nu(MnOC)/\nu_s(MnO_2)$ mode) to appear in the region around 980 cm^{-1} with an isotopic shift of 90 cm^{-1}, and the ν(MnO) vibration was calculated to absorb at around 650 cm^{-1} with medium intensity. However, no such bands are observed in the experimental spectrum, so that ^{3}**4** can be excluded as a product, too. According to the calculations, ^{3}**5**, ^{1}**6*** and the $MnO_2(OH)Cl$ part of **7** should be characterised by intense

  0947-6539/01/0721-4676 $ 17.50+.50/0 *Chem. Eur. J.* **2001**, *7*, No. 21

Table 1. Frequencies [cm^{-1}] obtained experimentally by the cocondensation of $Mn^{18}O_3Cl$ with a TME/Ar mixture (5%) and calculated frequencies (B3LYP, 6-311G(d); a scaling factor of 0.97 was applied) for ^{3}**1** and ^{3}**2** (intensities are given in parentheses). The assignments are based on the computational results.

$^{18}O_3$MnCl/TME	Exptl: $\Delta(^{16}O/^{18}O)$	Calcd: [^{18}O]-^{3}**1**	Calcd: $\Delta(^{16}O/^{18}O)$ for ^{3}**1**	Calcd: [^{18}O]-^{3}**2**	Calcd: $\Delta(^{16}O/^{18}O)$ for ^{3}**2**	Assignment
1483 (0.37)	0	1503 (0.08)	6			CH_3 bend
		1489 (0.14)	0	1493 (0.03)	0	
1464 (0.40)	0	1481 (0.04)	0	1481 (0.04)	0	
				1474 (0.02)	0	
				1472 (0.02)	0	CH_3 bend
1457 (0.37)	0	1455 (0.05)	0	1456 (0.07)	0	CH_3 bend
1448 (0.37)	0	1448 (0.05)	0	1449 (0.02)	0	CH_3 bend
1437 (0.30)		1406 (0.06)	0			
1393 (0.30)	0	1394 (0.09)	0	1394 (0.04)	0	CH_3 bend
1388 (0.97)	0	1389 (0.13)	0	1384 (0.10)	1	
1372 (0.50)	0	1366 (0.11)	1	1372 (0.10)	0	ν(CC)
1214 (0.37)	4	1189 (0.11)	1	1217 (0.02)	1	
1175 (0.90)	0	1167 (0.18)	0	1184 (0.11)	0	δ(CCC)
1115 (0.60)	5	1117 (0.27)	0	1149 (0.11)	1	ρ(CH_3)
1022 (0.22)	2	1013 (0.04)	2	1128 (0.38)	1	
				998 (1)	45	ν(Mn=O)
898 (1)	39	948 (1)	43			$\nu_{as}(MnO_2)$
				925 (0.13)	4	
				922 (0.06)	1	
				829 (0.81)	26	$\nu_{as}(MnO_2$, ring)
818 (0.47)	52	925 (0.32)	46			$\nu_s(MnO_2)$
				765 (0.07)	25	$\nu_s(MnO_2$, ring)
782 (0.62)	27	746 (0.82)	28			ν_s(COC)
				716 (0.27)	20	$\nu_{as}(MnO_2$, ring)/$\nu_{as}(C_2O_2)$
				667 (0.35)	24	$\nu_s(MnO_2$, ring)/$\nu_s(C_2O_2)$
		554 (0.16)	10			
489 (0.22)	15	512 (0.09)	20	459 (0.18)	9	
		421 (0.41)	4	447 (0.16)	1	ν(MnCl)
		397 (0.08)	13	394 (0.09)	6	

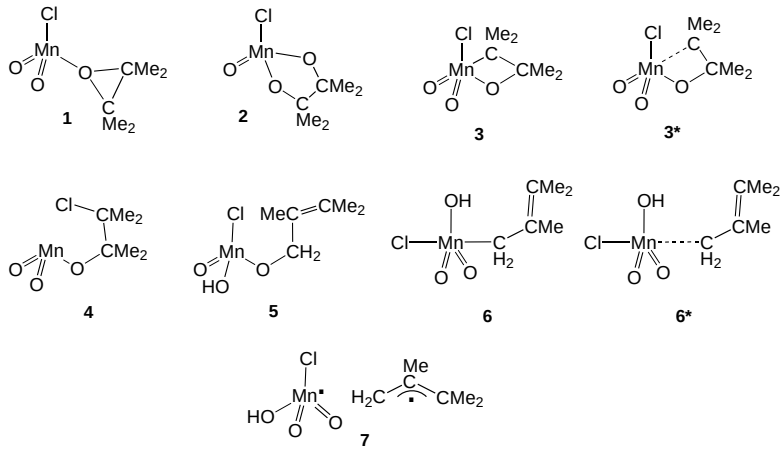

Scheme 2. Potential products of the reaction between MnO_3Cl and TME.

Table 2. Free reaction energies ΔG(293.15 K/0.001 atm) [kJ mol^{-1}] of the compounds **1**–**6** and **1a**–**3a** relative to the corresponding starting materials, as calculated by DFT [B3LYP/6–311G(d)]. ΔG(293.15 K/0.001 atm) for **7**, treated as two doublet radicals, is −215 kJ mol^{-1}.

	1	**2**	**3***	**4**	**5**	**6***	**1a**	**2a**	**3a**
singlet	−79	−161	+74	−47	−95	+21	−31	−152	–
triplet	−102	−217	–	−74	−154	–	−66	−203	+19

absorptions of the MnOH unit in the region around 600 cm^{-1}, but there is neither a band at this position (±150 cm^{-1}), nor is the fingerprint region of the experimental spectrum in agreement with an organic fragment $CH_2CMe{=}CMe_2$, and this is further evidence against the C–H activation products ^{3}**5**, ^{1}**6*** and **7**. This leaves only ^{3}**1** and ^{3}**2** as potential products, and their optimized structures are depicted in Figure 2.

The theoretical spectrum of ^{3}**2**, which would appear to be the most likely product by analogy with the permanganate ion (Scheme 1), and that of the epoxidation product ^{3}**1** are displayed in form of line diagrams in Figure 1. There are several arguments which point to an assignment to ^{3}**1**:

1) In agreement with the experiment, ^{3}**1** is predicted to show three bands with large $^{16}O/^{18}O$ isotopic shifts (the numbers on the lines in Figure 1): 948 (43), 925 (46) and 746 cm^{-1} (28 cm^{-1}), as opposed to ^{3}**2**, which should display five such bands.
2) As can be seen in Figure 1, the frequencies calculated for ^{3}**1** match the experimental values far better, and the intensity pattern is better reproduced, too. Comparatively large deviations (50 and 107 cm^{-1} after scaling) are only found for the $\nu_s(MnO_2)$ and $\nu_{as}(MnO_2)$ vibrations, as expected given the known tendency of B3LYP/6-311G(d) calculations to overestimate fundamental vibrations of metal–oxo compounds[37] (similar deviations are consequently also found for MnO_3Cl itself[38]). Here, the agreement between experiment and theory is better with the

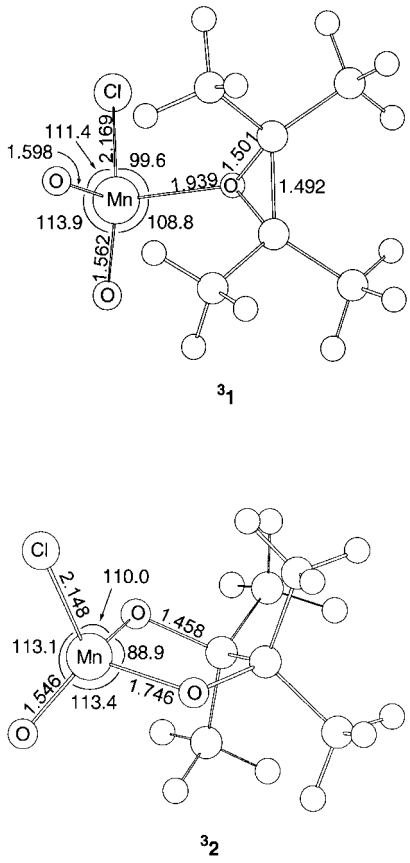

Figure 2. Structures of ^{3}**1** and ^{3}**2** as optimised by DFT methods (B3LYP/6–311G(d)) with bond lengths [Å] and angles [°].

LanL2DZ basis set (53 and 84 cm^{-1}, unscaled), but as this could not be later used for calculating the transition states, these results are not included in Figure 1 for reasons of consistency.

3) Even more importantly, the deviations of the isotopic shifts calculated for ^{3}**1** from those obtained experimentally are well within the acceptable range, while the rather large deviations in the case of ^{3}**2** cannot be explained. Furthermore, two additional medium-intensity bands were calculated for ^{3}**2** to appear at 716 and 667 cm^{-1}, while there are no bands at all present in the region between 780 and 550 cm^{-1} in the experimental spectrum.
4) To definitely distinguish between ^{3}**2** and ^{3}**1**, a decisive experiment with ^{16}O/^{18}O isotopically scrambled MnO_3Cl was performed. If the experimental band at 782 cm^{-1}, which appears at 809 cm^{-1} on using $^{16}O_3$MnCl, belonged to ^{3}**2** and not to ^{3}**1**, it would have to be assigned to one of the four vibrations calculated to absorb at 829, 765, 716 or 667 cm^{-1} with isotopic shifts of a comparable magnitude (20–30 cm^{-1}). According to the calculations all of these vibrations involve both O atoms of the glycolate ring; the employed mixture of $^{16}O_3$MnCl, $^{16}O_2{}^{18}O$MnCl and $^{16}O^{18}O_2$MnCl with a ratio of 1:1.8:1 should therefore lead to three IR spectroscopically distinguishable isotopic combinations for this glycolate ring (^{16}O/^{16}O, ^{16}O/^{18}O and ^{18}O/^{18}O with a ratio of 4.8:5.6:1). This means that for any of the four above-mentioned vibrations—and hence for the band at 782 cm^{-1} if it were assigned to one of them—a triplet would be expected on isotopic scrambling, that is, a band intermediate between 782 and 809 cm^{-1} should appear and have the highest intensity. The right-hand side of Figure 3 illustrates this hypothetical case for one of these vibrations. Since, however, the band at 782 cm^{-1} corresponds to the ring-stretching vibration of the epoxide ligand in ^{3}**1**, the above-mentioned isotopically scrambled mixture of MnO_3Cl species leads to only the two known bands at 809 and 782 cm^{-1} (as only one O atom is involved in the vibration) with an intensity ratio of 2:1 (Figure 3, left), and this lends further strong support to the assignment of the experimental spectrum to ^{3}**1**.
5) Finally, [^{18}O]TME complexed with O=$CrCl_2$ had already been found previously[23] to absorb at 788 cm^{-1} with an isotopic shift of 28 cm^{-1}, which is in excellent agreement with the present results.

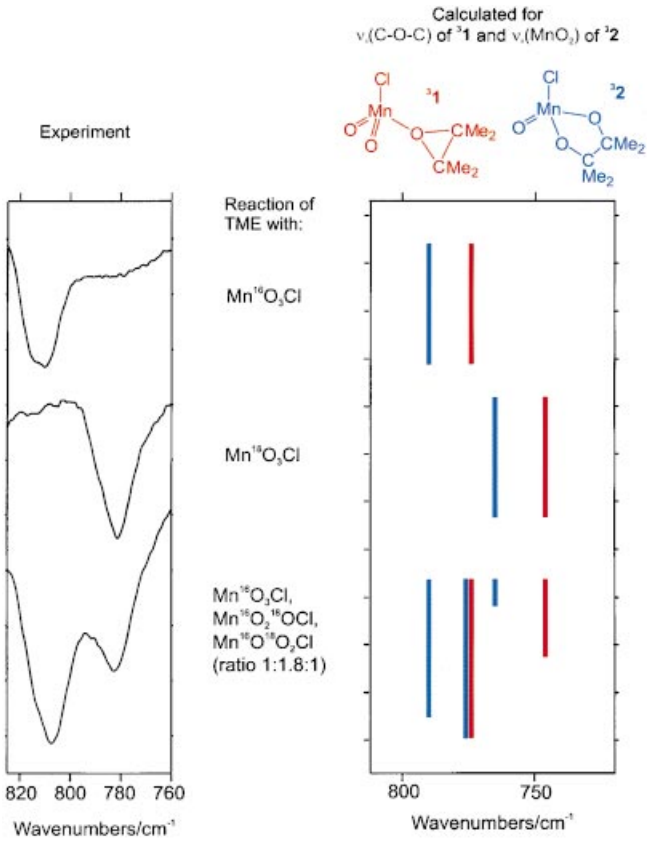

Figure 3. Left: the bands appearing at 809 cm^{-1} on using $^{16}O_3$MnCl and at 782 cm^{-1} on using $^{18}O_3$MnCl and their behaviour on employing a mixture of $^{16}O_3$MnCl, $^{16}O_2{}^{18}O$MnCl and $^{16}O^{18}O_2$MnCl with a ratio of 1:1.8:1. Right: the band pattern calculated (B3LYP/6-311G(d)) for the situations on the assumption that the band corresponds to ν_s(C-O-C) of ^{3}**1** and ν(MnO_2) of ^{3}**2**.

The intense bands of the experimental spectrum must therefore be assigned to ^{3}**1**. This does not necessarily mean that no ^{3}**2** is formed, since at low concentrations, most of its bands would be masked by those of ^{3}**1**. To determine an upper limit for the formation of ^{3}**2** relative to ^{3}**1**, we reconsidered the spectrum with regard to this aspect. A 1:1 mixture of the two compounds would give an overlap of the two theoretical spectra shown in Figure 1. If ^{3}**2** were present in the matrices, its most intense band should certainly be visible independ-

0947-6539/01/0721-4678 $ 17.50+.50/0 *Chem. Eur. J.* **2001**, *7*, No. 21

ently, but in close proximity to the most intense band of ^{3}**1** (898 cm^{-1}) on the high-energy side. Only one absorption can be observed there: a band at 926 cm^{-1}, whose integral ratio with respect to the band at 898 cm^{-1} is 1:13. If this band indeed belonged to ^{3}**2**, the corresponding additional absorptions calculated to appear at 925 and 829 cm^{-1} might be assigned to a weak band at 845 cm^{-1}, perturbed by subtraction of a band belonging to unconsumed MnO_3Cl, as well as a band which is almost completely covered by the band of ^{3}**1** at 809 cm^{-1}, respectively. Two medium-intensity absorptions remain for ^{3}**2**, with calculated frequencies of 716 and 667 cm^{-1}, and these could tentatively be correlated with two very weak bands at around 650 cm^{-1} which can be barely distinguished from the noise. On the basis of such assignments and the above-mentioned integration, a maximum of 7% of the converted TME can be estimated to yield ^{3}**2**, and 93% ^{3}**1**. This relative yield of 7% represents an upper limit, as there is no residual band in the experimental spectrum whose intensity exceeds the intensities of the bands discussed in this context.

It can therefore safely be concluded that, rather surprisingly, ^{3}**1** and not ^{3}**2** is the main reaction product (Scheme 3). In fact it is even quite certain that ^{3}**1** and not ^{1}**1** is formed: In the singlet state the two d electrons occupy a weakly antibonding Mn=O π^* orbital, while in the triplet state one of them occupies a more strongly antibonding Mn=O orbital; that is, the Mn=O bonds are stronger in the singlet state and absorb at much higher frequencies ($\Delta_{s/t}\nu$(Mn=O) is calculated to be

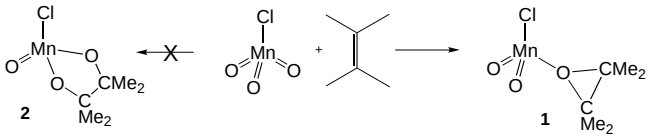

Scheme 3. Experimental outcome of the reaction between MnO_3Cl and TME.

to ca. 70 cm^{-1}). Consequently, the deviations of the band positions in the spectrum calculated for ^{3}**1** from the experimental absorptions are much smaller than those for ^{1}**1**, and hence the product must have been formed in its thermodynamically more stable triplet state.

The system MnO_3Cl/ethylene: thermodynamics and kinetics: Having identified ^{3}**1** as the main product of the MnO_3Cl/TME gas-phase reaction, the question arises why a [2+1] and not a [2+3] cycloaddition (as suggested for MnO_4^-) is the main reaction pathway. We hoped to gain more insights from DFT calculations of the thermodynamics and kinetics governing the reaction of MnO_3Cl with ethylene[39] to give **1a** and **2a**.

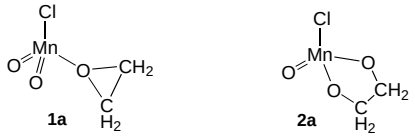

Scheme 4. The hypothetical ethylene-derived products ^{3}**1a** and ^{3}**2a**.

The triplet state of MnO_3Cl lies 86 kJ mol^{-1} higher in energy than the singlet state (in accordance with the formal d^0 configuration of the metal centre), and as the reaction was induced below room temperature, it is reasonable to assume that it starts from the singlet state. The reaction path of lowest energy leading to ^{3}**1a** involves a crossover from the singlet surface to the triplet surface immediately before the singlet transition state (TS) is reached from the reactant side (Figure 4).

First, the internal reaction coordinate (IRC) was traced starting from the TS of the singlet surface in both directions towards the starting materials in their singlet states and

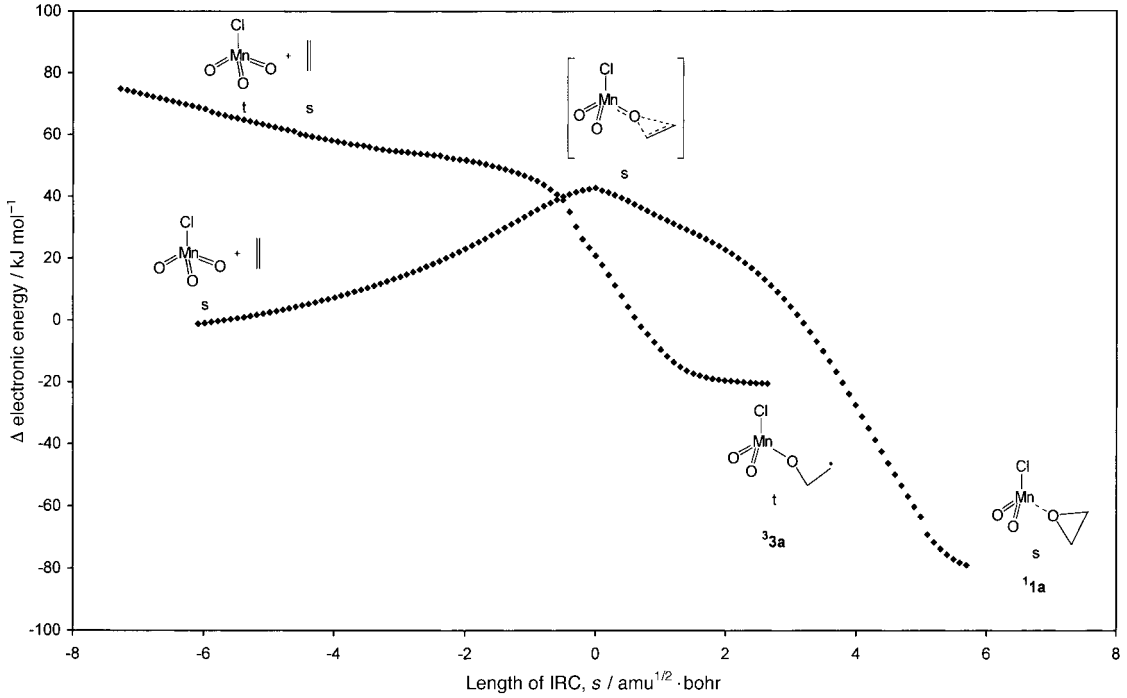

Figure 4. Energy profile for the reaction involving epoxidation of ethylene along the IRC path in the region where crossing of the two PESs occurs.

product ^{1}**1a** in steps of 0.1 amu$^{1/2}$bohr (Figure 4). Subsequently, the reaction between MnO_3Cl in its triplet state and ethylene was investigated: both compounds approach each other in an unsymmetric fashion to give the radical compound $(O)_2ClMnOCH_2CH_2^{\cdot}$ (^{3}**3a**) without passing through a TS (Figure 4). Compound ^{3}**3a** is a local minimum on the triplet surface that is separated from the product ^{3}**1a** by a barrier with a free enthalpy of only 19 kJ mol^{-1} (both the minimum (Figure 5) and the corresponding TS were optimised, and

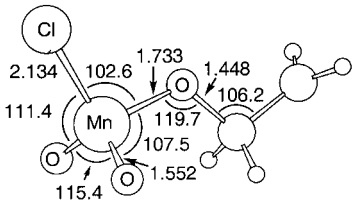

^{3}**3a**

Figure 5. Structure of ^{3}**3a** as optimised by DFT methods (B3LYP/6–311G(d)) with bond lengths [Å] and angles [°].

tracing the IRC showed that the TS is connected to both ^{3}**3a** and ^{3}**1a**, as shown in Figure 6, which plots the electronic energy. Intramolecular radical trapping by the terminal oxo ligands of $(O)_2ClMnOCH_2CH_2^{\cdot}$ to give ^{3}**2a**, which is also possible in principle, is prohibited by the rather large distance between these oxo ligands and the carbon-centred radical, as compared to the distance between the C-centred radical and the alkoxidic oxygen atom, which, in addition, has a higher spin density than the oxo O atoms. Compound ^{3}**1a** is 36 kJ mol^{-1} more stable than the corresponding product ^{1}**1a** on the singlet surface, and it therefore clearly represents the ground state of the product. Given this information on the singlet and triplet PESs, it was possible to locate their crossing point, where the singlet–triplet splitting is less than 0.1 kJ mol^{-1}. It is located just before the singlet TS, and thus the rate-determining activation barrier for the reaction of MnO_3Cl with ethylene to give ^{3}**1a** corresponds closely to the amount of energy required to surmount this singlet TS ($\Delta G^{\neq}$(293.15 K, 0.001 atm) = 102 kJ mol^{-1}; $\Delta E^{\neq}$ is calculated to be 43 kJ mol^{-1}; see Figures 7 and 4). The oxo-transfer process is not concerted: the two emerging C–O bonds are quite dissimilar at the point of intersection of the two PESs (Figure 8). Once this maximum has been reached on the singlet PES, the reaction can proceed along the triplet surface, passing the radical complex as a local minimum and finally reaching the triplet product ^{3}**1a** (Figure 7). Such crossing from singlet to triplet PESs can be facilitated under the adiabatic assumption by spin–orbit coupling.[24, 25]

Let us now turn to the [2+3] cycloaddition pathway. Compound ^{3}**2a** is 51 kJ mol^{-1} more stable than ^{1}**2a** and therefore represents the end point of the IRC. Furthermore ^{3}**2a** lies 137 kJ mol^{-1} lower in energy than ^{3}**1a**, so that its formation should indeed be thermodynamically favoured. However, thermodynamic control is excluded, since the interconversion of ^{3}**1a** and ^{3}**2a** is prohibited by substantial barriers (105/242 kJ mol^{-1}, see Figure 7). The TS between the starting materials and ^{3}**2a** (see Figure 9) is situated on the singlet surface, only 58 kJ mol^{-1} [$\Delta G^{\neq}$(293.15 K, 0.001 atm)] above the starting materials (spin crossover proceeds on the product side). In consequence, ^{3}**2a** appears to be not only the thermodynamically but also the kinetically favoured product.

The system MnO_3Cl/TME: thermodynamics and kinetics: Naturally, the enthalpies for the formation of the glycolate and epoxide complexes from reactions of MnO_3Cl with the olefinic bonds change to a certain extent on going from ethylene to TME: ΔG_f[^{3}**1a**/^{3}**2a**](293.15 K, 0.001 atm) is 22 kJ mol^{-1} larger than ΔG_f[^{3}**1**/^{3}**2**](293.15 K, 0.001 atm), and the reactions become more exothermic. According to the

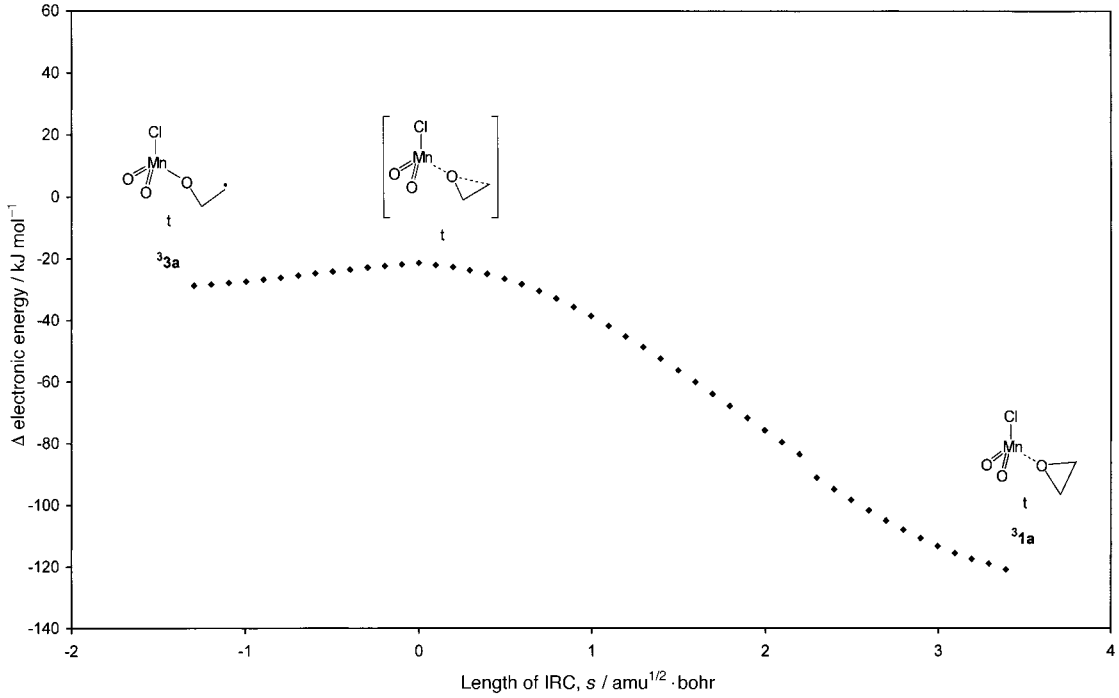

Figure 6. Energy profile for the conversion of the alkoxide radical $(O)_2ClMnCH_2CH_2^{\cdot}$ (^{3}**3a**) to the end product ^{3}**1a** along the IRC path.

0947-6539/01/0721-4680 $ 17.50+.50/0 *Chem. Eur. J.* **2001**, *7*, No. 21

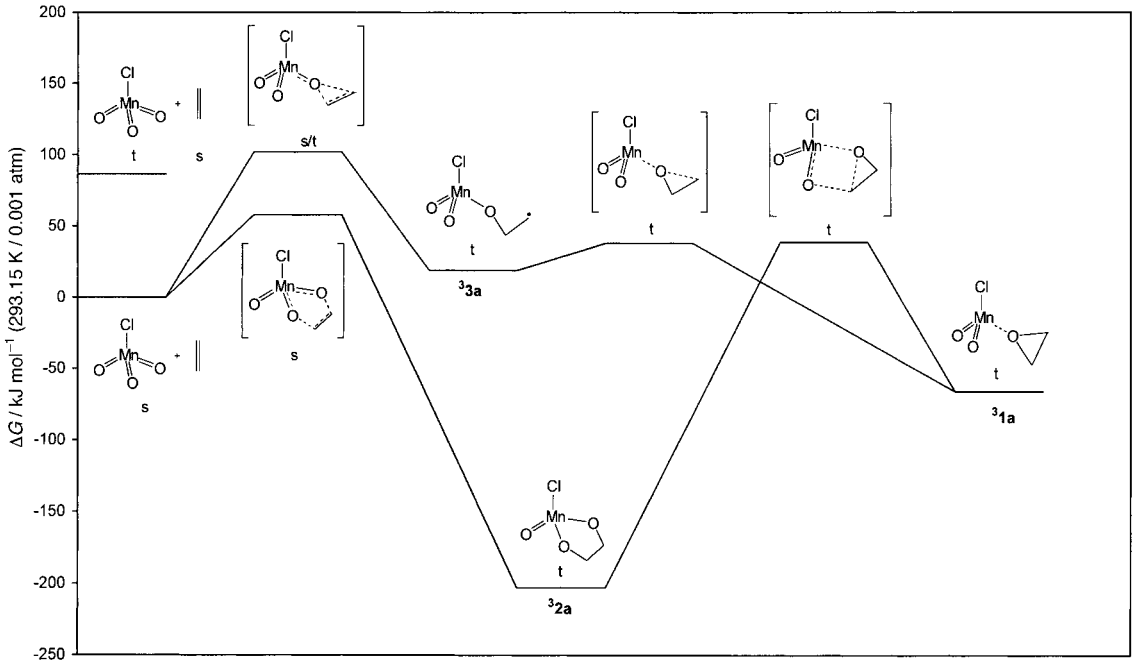

Figure 7. Reaction profile of the suggested mechanisms for the formation of ^{3}**1a** and ^{3}**2a** from MnO_3Cl and ethylene.

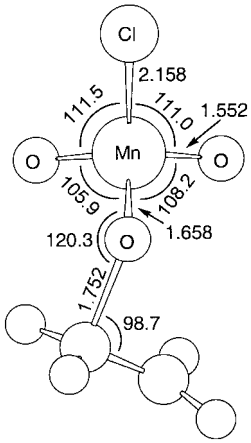

Figure 8. The structure of the rate-determining transition state for the epxidation of ethylene by MnO_3Cl, as optimised by DFT methods (B3LYP/6-311G(d)) with bond lengths [Å] and angles [°].

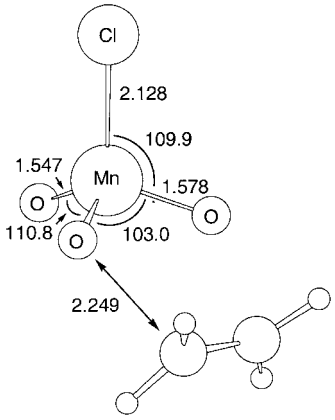

Figure 9. The structure of the rate-determining transition state for the [2+3] cycloaddition of ethylene to MnO_3Cl, as optimised by DFT methods (B3LYP/6–311G(d)) with bond lengths [Å] and angles [°].

results of Rösch et al.,[40] this means that the activation barrier for the [2+3] cycloaddition of TME is lower than that for ethylene, and a similar trend can also be expected for the epoxidation.

To analyse the influence of permethylation on these barriers more accurately, we performed further calculations, which were based on the results described above for ethylene. The rate-determining activation barrier for the epoxidation of ethylene by MnO_3Cl (resulting in ^{3}**1a**) corresponds closely to the energy of the corresponding TS on the singlet surface. Assuming that the same is true for TME,[39] we determined the structure and energy of the TS between the starting materials and ^{1}**1**. It is located only 45 kJ mol^{-1} above the starting materials, that is, the barrier is lowered by 57 kJ mol^{-1} on going from ethylene to TME, which represents an enormous substituent effect. This effect is less pronounced for the [2+3] cycloaddition, whose activation barrier was approximated[39] by monitoring the optimum energies for geometries in which TME approached MnO_3Cl symmetrically in five steps with fixed equally long O···C distances in a [2+3] fashion. It amounts to 45 kJ mol^{-1} (cf. 58 kJ mol^{-1} for ethylene), so that according to our calculations the barriers on the way to ^{3}**1** and ^{3}**2** are in fact numerically equal. Changing the basis sets or functionals used for the calculations is likely to change the calculated absolute (and to a smaller extent maybe even the relative) energies somewhat.[22–25, 30, 35, 36] Moreover, it has to be considered that we have made some approximations and assumptions[39] and that (as for any method) there are certain error ranges valid for results obtained by DFT methods. In an extreme case the epoxidation barrier could be overestimated by a few kJ mol^{-1}, while the cycloadditon barrier could be underestimated by a few kJ mol^{-1}, and this would lead to a kinetic control on the basis of these energy barriers. However, the fact that DFT calculations at a relatively high level of theory predicted the barriers to be of

an equal height must also be dealt with. This is the basis on which the question why MnO_3Cl reacts with TME selectively by direct epoxidation to give ^{3}**1** must be answered, even though this pathway is not favoured thermodynamically and there is no clear-cut kinetic reason (as far as the barriers are concerned) for the selective formation of ^{3}**1** rather than ^{3}**2**. Is a more constructive explanation available for the discrepancy between experimental and theoretical results than errors made by theory?

Reaction channels: In seeking an answer it is first necessary to consider the reaction conditions. The cocondensation of the two gases takes place at very low pressures (ca. 10^{-5} mbar), so that the mean free pathway of the molecules amounts to 1–2 cm. Since the common path followed the MnO_3Cl and TME gases after leaving their separate nozzles is only 2 cm, the molecules can collide only once or twice before condensation occurs, and these collisions will additionally not be very effective, because the beams flow almost parallel to one another and the MnO_3Cl molecules still have the thermal energy characteristic for a temperature of $-65\,^{\circ}C$. It is therefore unlikely that the molecules already react with each other in the gas phase. More collisions occur during the process of condensation on the CsI window, so that the reaction can proceed there, even though the molecules have already lost some of their thermal energy at that stage. This means that the activation barriers must be very low, even lower than those calculated above. Apparently the calculations overestimate these barriers, a finding which is not unusual, especially as the barriers were calculated for a temperature of 293.15 K, while the actual reaction probably takes place far below that temperature. However, for the present problem only relative trends, such as the fact that the barriers leading to ^{3}**1** and ^{3}**2** are of comparable magnitude, are of interest, and these should be reliable. Note, however, that calculated free activation enthalpies are not necessarily identical with those determined experimentally in kinetic investigations. The $\Delta E^{\neq}$ values can be reliably calculated for a specific two-dimensional reaction profile, and an evaluation of the calculated frequencies for the structures involved results in $\Delta G^{\neq}$ values like those discussed so far here. However, the real, measurable $\Delta G^{\neq}$ is determined by the three-dimensional PES, in which additional entropy contributions (which are disregarded in the corresponding partition function used in the calculation) can become important, for instance, the number of entrances a given system has to a particular path and their accessibility. Hence, the reaction channels should also be taken into account.

Formation of ^{3}**2** can only occur if the olefin approaches one MnO_2 unit rather symmetrically within its plane, so that the approach path for a successful reaction is quite narrow. There are three such planes, and therefore three reaction channels exist. A projection of these on a hemisphere is shown in Figure 10. In contrast, as outlined above, the reaction coordinate calculated for the epoxidation of ethylene revealed that the olefin is attacked unsymmetrically by one oxo group, so that there are many possible ways in which the olefin can approach the oxo ligands of MnO_3Cl and be epoxidised. The orbital interaction initialising the reaction will correspond to a four-electron/four-obital interaction[41] and the transition state structure shown in Figure 8 is of course just one possibility, in which the olefin approaches from the bottom side of the plane defined by the three oxo ligands. It can, however, also approach from above, and while entering it is also free to rotate around the C–O axis, which must subsequently be established as a bond in the TS. All this makes these reaction channels much broader than those of the [2+3] cycloaddition, and a corresponding projection on a hemisphere is shown in Figure 10. Epoxidation is thus statistically favoured over [2+3] cycloaddition. The latter practically requires frontal collision of the two molecules, while epoxidation could conceivably also occur in a less direct collision, that is, formation of ^{3}**1** is additionally supported by the higher efficiency of the collisions that lead to it. Nevertheless, some ^{3}**2** should be formed, too, and on the basis of our IR spectra 7% of the converted TME may indeed have reacted to give ^{3}**2** (vide supra). Compound ^{3}**1**, however, is clearly the main product. The fact that ethylene shows no reactivity can be explained in terms of the somewhat higher activation barriers (vide supra), which may be only just too high to be crossed during the process of condensation.

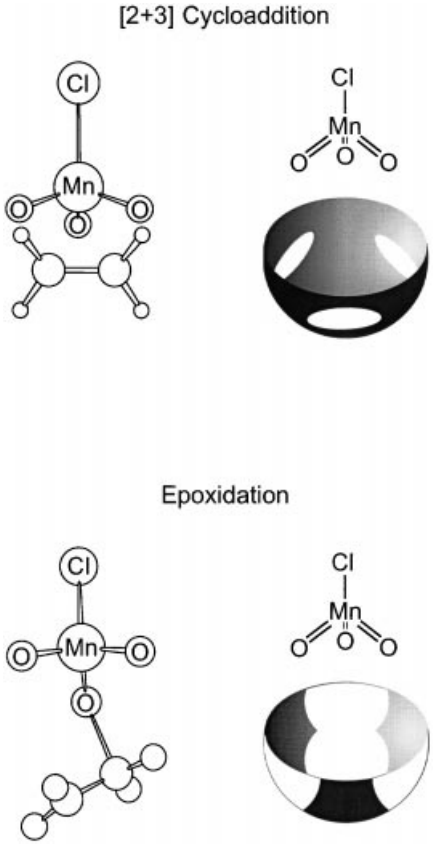

Figure 10. Reaction channels for the epoxidation and [2+3] cycloaddition with MnO_3Cl.

Behaviour of MnO_3Cl in solution: The above conclusions should still hold if the rather exotic "solvent" argon is replaced by a more common, but still relatively inert solvent. To test this hypothesis, we performed additional experiments on the reactivity of MnO_3Cl towards olefins in the liquid

0947-6539/01/0721-4682 $ 17.50+.50/0 *Chem. Eur. J.* **2001**, *7*, No. 21

phase. Epoxide complexes should again be the main primary products, although at somewhat higher temperatures interconversion to the more stable diolates could be expected if the corresponding barriers are low enough. According to the calculations, in the case of ethylene it is quite substantial (105 kJ mol^{-1}). Any of these primary products should undergo subsequent aggregation reactions leading to a solid, whose workup with polar, water-containing solvents provides the free organic oxidation products (epoxides or diols).

Treating *trans*-5-decene at $-80\,^{\circ}C$ with a solution of MnO_3Cl in $CFCl_3$ immediately leads to a suspension of a brown precipitate in a colourless solution. Workup with wet acetonitrile (at $-80\,^{\circ}C$ or after warming to room temperature) gave mainly *trans*-1,2-dibutyloxirane (37.5 %) in addition to the chlorinated[42] products *threo*-6-chlorodecan-5-ol (17.6 %; essentially free of *erythro* isomer), the corresponding 6-chlorodecan-5-one (36.1 %) and 5,6-dichlorodecane (8.8 %), as shown in GC/MS measurements by comparison with authentic samples (Scheme 5). Neither *threo*- or *erythro*-5,6-dihydoxodecane nor the products of their overoxidation, 6-hydroxydecan-5-one, 5,6-decanedione or valeric acid, could be detected. As MnO_3Cl already starts to decompose above $-30\,^{\circ}C$, it is impossible to weigh it without sacrifying part of it. This of course prohibits an accurate mass balance. The above products account for 60 % of the MnO_3Cl employed, which is satisfactory considering that a significant part of the MnO_3Cl would have decomposed already before it came into contact with the olefins and that the formation of some of the products can be assumed to require two equivalents of MnO_3Cl.

Our interest now focused on the oxidation of TME in solution, which can be compared directly with the reaction performed with the aid of the matrix isolation technique. Tetramethyethylene was shown previously to react quantitatively with the oxo groups of metal oxide chlorides,[23] probably because the individual steps relevant to oxygenation proceed faster due to the electron richness of the olefin, so that side reactions (e.g., chlorinations) are suppressed. When TME is treated with MnO_3Cl by the procedure described above, the epoxide is again obtained as the main product (77.2 %) together with the product of its Lewis acid catalysed rearrangement (pinacolone, 12.3 %) and some pinacol (10.4 %), probably resulting from epoxide hydrolysis. Consequently, **1**[3] is formed in solution as the main product, too, and this means that the epoxidation is again the preferred reaction pathway; this is additional support for the above interpretation.

A question remains: Why does MnO_4^- not epoxidise olefins? The present study showed that the seemingly analogous reaction of an olefin with MnO_4^- now must be considered as a completely different case, as the replacement of Cl^- by O^{2-} not only influences the singlet–triplet splitting, but also introduces an electronic charge. This leads to a situation in which, according to additional calculations, the epoxidation of ethylene by MnO_4^- is endothermic ($\Delta E = +53$ kJ mol^{-1}), while the [2+3] cycloaddition[30] is highly exothermic, as in the case of MnO_3Cl. Moreover, the negative charge leads to higher activation barriers, that is, to kinetic control, which, however, again favours the [2+3] cycloaddition. It is therefore understandable, that diols rather than epoxides are isolated from permanganate oxidations.

Conclusion

In summary, the high selectivity for the product ^{3}**1** has its origin, at least partly, in the greater number of approach paths for the olefin leading to ^{3}**1**, which are in addition much broader than those which yield ^{3}**2**. This situation leads to a statistical preference for the epoxidation path, which might be additionally favoured by lower requirements for the effectiveness of the corresponding collisions. It may also be that the epoxidation barrier is slightly lower than that of [2+3] cycloaddition, but we found no indication of this in our calculations. The present study thus provides precedent for the importance of considering all factors that guide a reaction so as be able to correctly predict an experimental result.

Product discrimination due to different approach paths, one of which is less accessible, might also provide an answer to the long-standing question why CrO_2Cl_2 epoxidizes olefins, while OsO_4 and MnO_4^- dihydroxylate them, although all these metal–oxo compounds should favour a [2+3] cycloaddition in the primary step according to calculations performed for ethylene.[17, 23–26, 30, 31] Currently we are investigating whether it is possible to design the matrix set-up in a way that allows even ethylene to react or that gives compound ^{3}**1** sufficient time and energy to rearrange to ^{3}**2** before the reaction mixture is quenched.

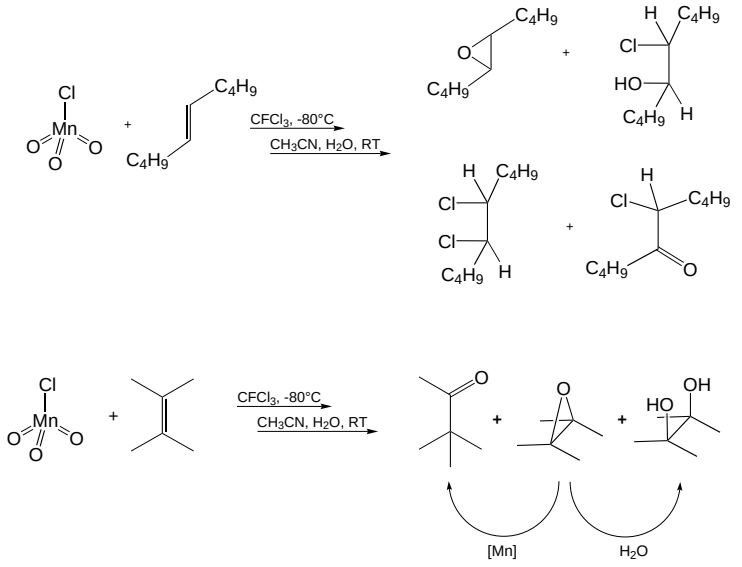

Scheme 5. Products obtained from the oxidation of *trans*-5-decene with MnO_3Cl after aqueous workup.

Experimental Section

Computational method: Density functional calculations were carried out with the Gaussian/DFT[43] series of programs. The B3LYP[44] formulation of density functional theory was used with the basis sets LanL2DZ and 6-311G(d). Harmonic vibrational frequencies and infrared intensities were predicted at these levels by numerical second derivatives by using analytically calculated first derivatives. All points were characterised as minima or first-order saddle points by frequency analysis.

Matrix-isolation experiments: Cooling by liquid helium gave temperatures of about 7 K inside a shroud maintained at a pressure below 10^{-7} mbar. Olefin/argon mixtures were prepared in a vacuum line by using standard manometric techniques and then deposited on the cold support. A CsI window was used for all the IR experiments and MnO_3Cl samples (held at $-65\,^{\circ}C$) were deposited continuously, typically over a period of 20 min; the rate of deposition of the material to be isolated was regulated by its own low volatility at that temperature.

IR spectra were recorded in transmission mode in the range of 4000–300 cm^{-1} and with a resolution of 1 cm^{-1} on a Bruker IFS 88 v spectrophotometer.

Starting materials: Tetramethylethylene (99% pure) was supplied by Aldrich and further purified by fractional condensation in high vacuum prior to use. Argon (99.999% pure) was supplied by Messer Griesheim. ^{18}O-Enriched MnO_3Cl was prepared by a procedure published for MnO_3F.[45] Isotopically scrambled MnO_3Cl was prepared by heating a solution of $KMnO_4$ in $H_2{}^{16}O/H_2{}^{18}O$ for 60 h at 100 °C. After removal of the volatile substances, as-prepared material was employed for the synthesis of MnO_3Cl.[32d]

Solution experiments: In a typical experiment MnO_3Cl (0.045 g, 0.325 mmol) was condensed into a flask equipped with a greaseless tap, $CFCl_3$ (20 mL) was cocondensed and the mixture was warmed to $-80\,^{\circ}C$. It was subsequently cocondensed onto a frozen ($-196\,^{\circ}C$) mixture of a 1.5 molar excess of the olefin and $CFCl_3$ (20 mL). After warming the reaction vessel to $-80\,^{\circ}C$ with stirring, the solution immediately turned colourless, and a brown solid precipitated. The suspension was stirred at $-80\,^{\circ}C$ for 1 h and at room temperature for 1 h. All volatile substances were removed and investigated by GC/MS with a standard to give a mass balance. They contain unconverted olefin and epoxide. The brown residue was treated with wet acetonitrile, and again all volatile substances were removed and investigated by GC/MS. They contained epoxide, carbonyl compounds and chlorinated products.

Authentic samples of the isomers of 5,6-decanediol were prepared by treatment of *trans*-5-decene with OsO_4 and subsequent aqueous workup, as well as by acid/base-catalysed hydrolysis of *trans*-1,2-dibutyloxirane. Samples of 6-hydroxydecane-5-one, 5,6-decanedione and valeric acid were obtained by reaction of *trans*-5-decene with an excess of $KMnO_4$. Epoxides were generally synthesised by oxidation of the olefins with *m*-chloroperbenzoic acid. *erythro*-6-Chlorodecan-5-ol can be synthesised by opening the corresponding epoxide with HCl, and 5,6-dichlorodecane is the main product when the olefin is treated with Cl_2.

Acknowledgement

This work was supported by the Deutsche Forschungsgemeinschaft (Habilitanden and Heisenberg scholarships to C.L. and financial support by the SFB 247), the Fonds der Chemischen Industrie and the Dr. Otto Röhm Gedächtnisstiftung.

[1] R. H. Holm, *Chem. Rev.* **1987**, *87*, 1401; R. H. Holm, *Coord. Chem. Rev.* **1990**, *100*, 183.
[2] W. A. Nugent, J. M. Mayer, *Metal–Ligand Multiple Bonds*, Wiley, New York, **1988**; L. K. Woo, *Chem. Rev.* **1993**, *93*, 1125; R. H. Holm in *Bioinorganic Catalysis* (Ed.: J. Reedijk), Marcel Dekker, New York, **1993**, pp. 347–393; K. B. Sharpless, *Tetrahedron* **1994**, *50*, 4235, and references therein; E. N. Jacobsen, L. Deng, Y. Furukuwa, L. Martinez, *Tetrahedron* **1994**, *50*, 4324, and references therein.
[3] J. H. Enemark, C. G. Young, *Adv. Inorg. Chem.* **1993**, *40*, 1.
[4] *Organic Synthesis by Oxidation with Metal Compounds* (Eds.: W. Mijs, C. R. H. I. de Jonge), Plenum, New York, **1986**.
[5] H. K. Singh in *Cytochrome P-450: Structure, Mechanism, and Biochemistry* (Ed.: R. R. Ortiz de Montellano), 2nd ed., Plenum, New York, **1995**; A. E. Shilov, A. A. Shteinman, *Acc. Chem. Res.* **1999**, 32, 763.
[6] G. Cainelli, G. Cardillo, *Chromium Oxidations in Organic Chemistry*, Springer, Berlin, **1984**; K. B. Wiberg in *Oxidation in Organic Chemistry* (Ed.: K. B. Wiberg), Academic Press, New York, **1965**, 69.
[7] F. H. Westheimer, *Chem. Rev.* **1949**, *49*, 419; F. Freeman in *Organic Syntheses by Oxidation with Metal Compounds* (Ed.: W. J. Mijs, C. R. H. I. de Jonge), Plenum, New York, **1986**, Chap. 2, pp. 41.
[8] a) K. B. Sharpless, K. Akashi, *J. Am. Chem. Soc.* **1975**, *97*, 5927; b) K. B. Sharpless, T. C. Flood, *J. Am. Chem. Soc.* **1971**, *93*, 2316; L. M. Hjelmeland, G. H. Loew, *J. Am. Chem. Soc.* **1977**, *99*, 3514; review: M. Schröder, *Chem. Rev.* **1980**, *80*, 187.
[9] C. Döbler, G. M. Mehltretter, U. Sundermeier, M. Beller, *J. Am. Chem. Soc.* **2000**, *122*, 10289.
[10] F. A. Carey, R. J. Sundberg, *Advanced Organic Chemistry*, Plenum Press, New York, **1977**.
[11] G. L. Lee, T. Chen, *J. Org. Chem.* **1991**, *56*, 5341, and references therein; G. L. Lee, T. Chen, *J. Am. Chem. Soc.* **1993**, *115*, 11231.
[12] W. A. Waters, *Quart. Rev.* **1958**, *12*, 29; H. B. Henbest; W. R. Jackson, B. C. G. Robb, *J. Chem. Soc B* **1966**, 803.
[13] K. B. Sharpless, A. Y. Teranishi, J.-E. Bäckvall, *J. Am. Chem. Soc.* **1977**, *99*, 3120.
[14] G. Wagner, *J. Russ. Phys. Chem. Soc.* **1895**, *27*, 219; K. B. Wiberg, K. A. Saegebarth, *J. Am. Chem. Soc.* **1957**, *79*, 2822.
[15] K. A. Jørgensen, R. Hoffmann, *J. Am. Chem. Soc.* **1986**, *108*, 1867.
[16] M. Sono, M. P. Roach, E. D. Coulter, J. H. Dawson, *Chem. Rev.* **1996**, *96*, 2841.
[17] $LReO_3$: D. V. Deubel, G. Frenking, *J. Am. Chem. Soc.* **1999**, *121*, 2021; M. A. Pietsch, T. V. Russo, R. B. Murphy, R. L. Martin, A. K. Rappé, *Organometallics* **1998**, *17*, 2716; S. Köstlmeier, V. Nasluzov, W. A. Herrmann, N. Rösch, *Organometallics* **1997**, *16*, 1786.
[18] CrO_2Cl_2/C–H: G. K. Cook, J. M. Mayer, *J. Am. Chem. Soc.* **1994**, *116*, 1855; G. K. Cook, J. M. Mayer, *J. Am. Chem. Soc.* **1995**, *117*, 7139.
[19] MnO_4^-/C–H: K. A. Gardner, J. M. Mayer, *Science* **1995**, *269*, 1849; K. A. Gardner, L. L. Kuehnert, J. M. Mayer, *Inorg. Chem.* **1997**, *36*, 2069.
[20] J. M. Mayer, *Acc. Chem. Res.* **1998**, *31*, 441.
[21] Reactions of metal–oxo compounds in the gas phase: S. Shaik, M. Filatov, D. Schröder, H. Schwarz, *Chem. Eur. J.* **1998**, *4*, 193; D. Schröder, H. Schwarz, S. Shaik, *Struct. Bonding* **2000**, *97*, 91; D. Schröder, S. Shaik, H. Schwarz, *Acc. Chem. Res.* **2000**, *33*, 139; P. Jackson, J. N. Harvey, D. Schröder, H. Schwarz, *Int. J. Mass Spect.* **2001**, *204*, 233.
[22] CrO_2Cl_2/olefin: C. Limberg, R. Köppe, H. Schnöckel, *Angew. Chem.* **1998**, *110*, 512; *Angew. Chem. Int. Ed.* **1998**, *37*, 496.
[23] CrO_2Cl_2/olefin: C. Limberg, R. Köppe, *Inorg. Chem.* **1999**, *38*, 2106.
[24] CrO_2Cl_2/olefin: M. Torrent, L. Deng, T. Ziegler, *Inorg. Chem.* **1998**, *37*, 1307.
[25] CrO_2Cl_2/olefin: M. Torrent, L. Deng, M. Duran, M. Solá, T. Ziegler, *Can. J. Chem.* **1999**, *77*, 1476.
[26] OsO_4/olefin: a) S. Dapprich, G. Ujaque, F. Maseras, A. Lledós, D. G. Musaev, K. Morokuma, *J. Am. Chem. Soc.* **1996**, *118*, 11660; b) U. Pidun, C. Boehme, G. Frenking, *Angew. Chem.* **1996**, *108*, 3008; *Angew. Chem. Int. Ed. Engl.* **1996**, *35*, 2817; c) M. Torrent, L. Deng, M. Durun, M. Solà, T. Ziegler, *Organometallics* **1997**, *16*, 13; d) A. J. Del Monte, J. Haller, K. N. Houk, K. B. Sharpless, D. A. Singleton, T. Strassner, A. A. Thomas, *J. Am. Chem. Soc.* **1997**, *119*, 9907.
[27] CrO_2Cl_2/MeOH: a) T. Ziegler, J. Li, *Organometallics* **1995**, *14*, 214; b) L. Deng, T. Ziegler, *Organometallics* **1997**, *16*, 716.
[28] CrO_2Cl_2/MeOH: B. S. Ault, *J. Am. Chem. Soc.* **1998**, *120*, 6105.
[29] K. N. Houk, T. Strassner, *J. Am. Chem. Soc.* **2000**, *122*, 800.
[30] a) K. N. Houk, T. Strassner, *J. Org. Chem.* **1999**, *64*, 800; b) T. Strassner, M. Busold, *J. Org. Chem.* **2001**, *66*, 672.
[31] C. Limberg, *Chem. Eur. J.* **2000**, *6*, 2083.
[32] a) J. Dumas, *Ann. Chim. Phys.* **1827**, *36*, 81/2; b) B. Aschoff, *Chem. Zentral.* **1860**, *31*, 838; B. Aschoff, *Monatsber. Kgl. Preuß. Akad. Wiss. Berlin* **1860**, *474*/85, *483*/5; c) B. Franke, *J. Prakt. Chem.* **1887**, *36*, 31; d) T. S. Briggs, *J. Inorg. Nucl. Chem.* **1968**, *30*, 2866.

  0947-6539/01/0721-4684 $ 17.50+.50/0

[33] R. M. E. Vliek, P. R. Boudewijn, P. J. Zandstra, *Chem. Phys. Lett.* **1976**, *39*, 405; E. Diemann, E. L. Varetti, A. Müller, *Chem. Phys. Lett.* **1977**, *51*, 460; P. J. Aymonino, H. Schulze, A. Müller, *Z. Naturforsch. B* **1969**, *24*, 1508; J. Jasinski, S. L. Holt, *J. Chem. Soc.* **1972**, 1046; E. L. Varetti, A. Müller, *Z. Anorg. Allg. Chem.* **1978**, *442*, 230; J. P. Jasinski, S. L. Holt, J. H. Wood, J. W. Moskowitz, *J. Chem. Phys.* **1975**, *63*, 1429; S. Rettrup, S. Bo, C. J. Ballhausen, *Acta Chem. Scand.,* **1990**, *44*, 853.

[34] The optical properties of matrices thus obtained are not as good as those of matrices generated by prior matrix isolation of a given substrate followed by a subsequent photolytically induced reaction. Hence, the bands in the IR spectra of such matrices are comparatively broad.

[35] M. Torrent, P. Gili, M. Duran, M. Solà, *J. Chem. Phys.* **1996**, *104*, 9499.

[36] A.Bérces, T. Ziegler, *J. Phys. Chem.* **1995**, *99*, 11417; A. Bérces, *J. Phys. Chem.* **1996**, *100*, 16538.

[37] I. Bytheway, M. W. Wong, *Chem. Phys. Lett.* **1998**, *282*, 219.

[38] Vibrational frequencies [cm^{-1}] of MnO_3Cl (experimental[33] versus calculated [B3LYP/6–311G(d), scaling factor of 0.97]): $\nu_{as}(MnO_3)$ 951.5 versus 1064.6, $\nu_{as}(MnO_3)$ 889.9 versus 1012.3, ν(MnCl) 458.9 versus 468.0.

[39] The detailed investigation of the TME system is computationally very demanding.

[40] The activation energies of [2+3] cycloadditions between olefins and metal oxo moieties can be correlated with the reaction energies on the basis of Marcus theory: P. Gisdakis, N. Rösch, *J. Am. Chem. Soc.* **2001**, *123*, 697.

[41] The oxidation must involve both the HOMO and LUMO of the oxidant, as well as the HOMO and LUMO of the olefin.[18, 19] The HOMO of MnO_3Cl is primarily an oxygen lone pair.

[42] The source of chlorine is not entirely clear for some of the products. Dichlorination is probably due to partial decomposition of MnO_3Cl to give free Cl_2. Abstraction of Cl from the solvent $CFCl_3$ by intermediate alkoxide radicals (analogous to **3a**, vide supra) is also conceivable.

[43] Gaussian 98, Revision A.6, M. J. Frisch, G. W. Trucks, H. B. Schlegel, G. E. Scuseria, M. A. Robb, J. R. Cheeseman, V. G. Zakrzewski, J. A. Montgomery, Jr., R. E. Stratmann, J. C. Burant, S. Dapprich, J. M. Millam, A. D. Daniels, K. N. Kudin, M. C. Strain, O. Farkas, J. Tomasi, V. Barone, M. Cossi, R. Cammi, B. Mennucci, C. Pomelli, C. Adamo, S. Clifford, J. Ochterski, G. A. Petersson, P. Y. Ayala, Q. Cui, K. Morokuma, D. K. Malick, A. D. Rabuck, K. Raghavachari, J. B. Foresman, J. Cioslowski, J. V. Ortiz, B. B. Stefanov, G. Liu, A. Liashenko, P. Piskorz, I. Komaromi, R. Gomperts, R. L. Martin, D. J. Fox, T. Keith, M. A. Al-Laham, C. Y. Peng, A. Nanayakkara, C. Gonzalez, M. Challacombe, P. M. W. Gill, B. Johnson, W. Chen, M. W. Wong, J. L. Andres, C. Gonzalez, M. Head-Gordon, E. S. Replogle, J. A. Pople, Gaussian, Inc., Pittsburgh PA, **1998**.

[44] A. D. Becke, *J. Chem. Phys.* **1993**, *98*, 5648.

[45] E. L. Varetti, R. R. Filgueira, A. Müller, *Spectrochim. Acta*, **1981**, *37A*, 369.

Received: January 30, 2001
Revised: June 20, 2001 [F3037]